International Journal of Mechanical Sciences 205 (2021) 106604

Contents lists available at ScienceDirect

International Journal of Mechanical Sciences

journal homepage: www.elsevier.com/locate/ijmecsci

Microcapsule mechanics: Quasi-static compressive properties and the effect of liquid core

Yunxiao Zhang [a], Ying Zhao [a], Fang Wu [b], Xin Zhang [c], Zhong Zhang [d], Yong Xiang [b,*], Jinglei Yang [a,*]

[a] Department of Mechanical and Aerospace Engineering, Hong Kong University of Science and Technology, Clear Water Bay, Kowloon, Hong Kong, PR China
[b] School of Materials and Energy, University of Electronic Science and Technology of China, Chengdu, PR China
[c] Department of Mechanics and Aerospace Engineering, Southern University of Science and Technology, Shenzhen, Guangdong 518055, PR China
[d] CAS Key Laboratory of Nanosystem and Hierarchical Fabrication, CAS Center for Excellence in Nanoscience, National Center for Nanoscience and Technology, Beijing 100190, PR China

ARTICLE INFO

Keywords:
Microcapsules
Young's modulus
Shell
Liquid core
Deformation

ABSTRACT

Liquid-filled microcapsules with a core-shell structure have been developed and widely applied in multi-functional materials. Mechanical properties of microcapsules play a vital role in production, collection and re-processing. Nevertheless, their mechanical behaviors have not been comprehensively understood. In this study, poly urea-formaldehyde (PUF) shelled microcapsules with paraffin oil are selected for experiments. Intrinsic mechanical properties of the shell material obtained from nanoindentation test and uniaxial compression test show remarkably good consistence. Both experimental and simulation results unprecedentedly reveal that the liquid core has a significant effect on the mechanical properties of a microcapsule by enhancing the stability and facilitating the stretching of the shell under compression, especially at large deformations. Moreover, the relationship between the rising hydrostatic pressure and the structural deformation is found to nicely follow up a quadratic function. When the structural deformation increases, plasticity successively appear at the circular contact area, contact edge, and non-contact area of the shell.

1. Introduction

Since Jong and Bonner [1,2] synthesized the first artificial microcapsules in the 1930s, various microcapsules were designed and fabricated in labs and have found many applications in printing, food industry, cosmetics, pharmacy and novel materials for self-healing, self-lubricating and self-cleaning [3–7]. The core-shell microcapsules containing a liquid core are usually encapsulated by a single layer or multi-layers organic or inorganic shell. The functional core materials are supposed to be delivered to the right place at the right time. Before the release of the liquid core material occurs, the solid shell can provide crucial protection to remain the stability and integrity of microcapsules during manufacturing, processing, transportation, and application. Microcapsules suffer different loads while being mixed with matrix materials such as epoxy during reprocessing. The failure of microcapsules can be triggered by external mechanical stimulation or internal osmotic pressure [8]. Hence, it is essential to investigate their mechanical properties to better control their quality and tailoring properties as prospected.

A variety of microcapsules have been successfully fabricated with different shell materials [9,10]. The selection of shell materials depends on several factors, including the reactivity of the core material, the release requirements in applications, and compatibility with synthesis methods. During the past decades, a number of encapsulation methods have been developed and applied in diverse fields [10]. As a microcapsule has a composite structure, both physical properties of the shell and the core material can significantly affect that of the whole structure. Most researchers studied microcapsule mechanics through compression tests [11–14]. Among the experimental techniques used to obtain the force-displacement data during compression on individual microcapsules, atomic force microscopy (AFM) [15–17], nanoindentation [18–21] and micromanipulation technique [22–26] have been widely adopted for many years.

To analyze the experimental data, elastic contact mechanics and shell theory were introduced for core-shell structure. In 1882, based on continuum mechanics and elasticity theory, Hertz [27] solved the contact problem of two elastic bodies with curved surfaces. The contact

* Corresponding author.
E-mail addresses: xiang@uestc.edu.cn (Y. Xiang), maeyang@ust.hk (J. Yang).

https://doi.org/10.1016/j.ijmecsci.2021.106604
Received 7 April 2021; Received in revised form 8 June 2021; Accepted 14 June 2021
Available online 19 June 2021

force F is given by

$$F = \frac{4}{3}\sqrt{R_0}E_r\Delta^{3/2} \tag{1}$$

where R_0 is the effective radius of the contact and defined as

$$\frac{1}{R_0} = \frac{1}{R_1} + \frac{1}{R_2} \tag{2}$$

R_1 and R_2 are the radii of the two contact bodies. Δ is the total normal deflection. E_r is the effective stiffness related to the elastic properties of the materials. Thus,

$$\frac{1}{E_r} = \frac{1-\upsilon_1{}^2}{\mathrm{E}_1} + \frac{1-\upsilon_2{}^2}{\mathrm{E}_2} \tag{3}$$

where E_1, E_2 are the Young's modulus and υ_1, υ_2 are the Poisson's ratio of the two bodies. Contact area and distributed normal pressure are also derived. Thereafter the assumptions of Hertz model were discussed by researchers [28–31]. In 1971, Johnson et al. [32] investigated the adhesion effect in lightly loaded contacts of solids and modified Hertz equations. For a shallow spherical empty shell (h/R « 0.1) subjected to a point load, Reissner [33] predicted the bending force at a small deformation (d/h « 0.1) as

$$F = \frac{4}{\sqrt{3(1-\nu^2)}}\frac{Eh^2}{R}d \tag{4}$$

where E, ν are the Young's modulus and Poisson's ratio of the shell respectively, h is the shell thickness and d is the indentation depth. Reissner's model accounts for the bending of the shell, which dominates in small deformations. Although both models have been successfully applied in previous work [13], their limitations cannot be neglected. The Hertz model and shell theory solve the problem in the elastic regime with small deformations [34]. In real experiments, the tested materials and loading conditions may deviate from the assumptions. The existence of friction, adhesion effect, large deformations, plasticity, time-dependent effect, and core effect [35] can lead to erroneous results. Thus, it is important to deeply investigate the mechanical response of a microcapsule with a core-shell structure and discuss the applicability of traditional models in microcapsule mechanics.

During the past few decades, researchers endeavored to extract the intrinsic mechanical parameters of individual microcapsules, including Young's modulus and failure stress. The deformation and failure mechanism of individual microcapsules have attracted the most interests. Keller et al. [36] found that the average Young's modulus of PUF shell was 3.7 GPa and smaller microcapsules showed higher failure strength. Yang et al. [37] synthesized polyurethane microcapsules and their results suggested that the failure strength decreased exponentially with diameter. For the rupture of a compressed microcapsule, brittle and ductile scenarios have been observed. The silica shell microcapsules were reported to exhibit brittle rupture [20] characteristic. The failure stress for a tetraethoxyorthosilane-methyltrimethoxysilane microcapsule that ruptured near the elastic regime was estimated to be $11 - 14 \pm 10$ MPa [22]. Before the initial crack occurs, the shell material probably has already yielded due to excessive local stresses. The calculated yield strength of the melamine-formaldehyde (MF) microcapsule was about 130 MPa based on an elastic-perfectly plastic assumption of the wall material [38]. Though the apparent mechanical response of the core-shell structure has been analyzed, the core effect is usually ignored for simplification. It is therefore necessary to further reveal the relationship between the structure and mechanical properties of a single microcapsule.

Finite element method (FEM) has shown its potential in simulating the deformation and stress evolution of a compressed microcapsule. Through the comparison of experimental loading curves and numerical results, key mechanical parameters can be estimated. Mercadé-Prieto et al. [39] successfully calculated the ratio of wall thickness to microcapsule radius h/R and Eh. Ghaemi et al. [40] concluded that the failure in the meridian direction of a compressed microcapsule was caused by circumferential stress. Zhang et al. [41] studied the rate dependent behaviors of nickel-based microcapsules and predicted the crack generation in the shell which showed good agreement with experimental observations. The liquid core was usually modelled as solid or incompressible [22,25,41,42]. While the compression of a microcapsule is a fluid-structure interaction problem, the liquid core should be modelled properly to better understand the core effect in microcapsule mechanics.

In this study, poly urea-formaldehyde is synthesized to encapsulate paraffin oil. Nanoindentation test is conducted on shell fragments to obtain the elastic modulus. The FEM results are compared with quasi-static compression data on single microcapsules. The deformation mechanism, stress evolution and liquid core effect of the core-shell structure are discussed.

2. Materials and methods

2.1. Synthesis of poly urea-formaldehyde microcapsules

In the present work, PUF microcapsules were synthesized by an *in situ* polymerization method with chemicals used without further purification unless otherwise specified. The urea-formaldehyde prepolymer was synthesized first in a typical way [43]. 27.5 g aqueous solution of formaldehyde (37 wt.%, Sigma-Aldrich) was adjusted to pH 8.0 with 1 mol^{-1} NaOH solution and then 10.2 g urea (Sigma-Aldrich) was dissolved to the obtained solution in a 250 ml beaker. The mixture was then suspended in a 70 ˚C water bath for 60 min under magnetic stirring of 1000 rpm. A urea-formaldehyde prepolymer aqueous solution was obtained after the reaction. Then 12.5 g surfactant ethylene-maleic anhydride (EMA, Sigma-Aldrich) aqueous solution together with 50 ml deionized water was added to the prepolymer solution in a 600 ml beaker. The mixture was agitated using a digital mixer (Caframo) driving a three-bladed propeller at a rate of 1000 rpm at 22 ˚C. 10 g paraffin oil dyed with Sudan III was poured into the beaker slowly. After emulsification for 15 min, the pH of the solution was adjusted to pH 2.0 with an aqueous solution of citric acid (50 wt.%). The reaction was terminated after 2 h and it was cooled to room temperature. The collected PUF microcapsules were rinsed with deionized water for 5 times, filtered and air-dried under room temperature for 12 h before further tests.

2.2. Preparation of the specimen for nanoindentation test

0.2 g PUF microcapsules containing paraffin oil were mixed with 4.0 g epoxy resin and 1.3 g curing agent (Epolam 5015, Sika). After agitation, the suspension was degassed using a vacuum oven for 30 min. The suspension was poured slowly into a cylindrical mold. After 72 h of 50 ˚C heating, the epoxy resin was fully cured. The end surface of the specimen was polished. During polishing, the microcapsules were broken and only half part of the shell remained embedded in the epoxy matrix. Hexane (Sigma-Aldrich) was used to remove the residual paraffin oil.

2.3. Nanoindentation using a Berkovich indenter

Nanoindentation tests were performed using a TI 900 Triboindenter (HYSITRON Inc., USA). The exposed inner surface of the PUF shell fragment was imaged and probed with a Berkovich tip. The maximum displacement is 200 nm, about one tenth of the shell thickness [44,45]. To minimize the time-dependent effect during probing, the tip was held for 10 s after the displacement reached the maximum value. The Young's modulus was determined from analyzing the obtained force-displacement curve based on the Oliver-Pharr method [46,47]. This method expresses the slope of the initial linear unloading portion (S) as a function of the reduced modulus of elastic contact (E_r) and projected area of contact (A_c) at the peak load. The modulus of the specimen can be computed from

$$S = \frac{dP}{dh} \tag{5}$$

$$E_r = \frac{\sqrt{\pi}}{2\beta} \times \frac{S}{\sqrt{A_c}} \tag{6}$$

$$\frac{1}{E_r} = \frac{1-\nu^2}{E} + \frac{1-\nu_i{}^2}{E_i} \tag{7}$$

where E, ν are the Young's modulus and Poisson's ratio of the specimen respectively, and E_i (1140 GPa), ν_i (0.07) are the counterparts of the indenter. β is 1.034 for the Berkovich indenter. ν is acceptably assumed to be 0.33 [36]. As the modulus of the indenter is much higher than that of the tested material, the reduced modulus E_r is only related to the mechanical properties of the fabricated poly urea-formaldehyde.

2.4. Compression on single PUF microcapsules

A setup [36] was established for compression tests on single microcapsules. The sample was mounted on a substrate and compressed by a flat plate connected to a 20 g loadcell (FSH02666, Futek), driven by an actuator (GTS70, Newport) at a preset speed of 1 μm/s. The resolution of the actuator and loadcell is 0.1 μm and 0.003 mN, respectively. A CCD camera with a 35X close focus dual purpose lens was used to take real-time images of the deformed sample during compression. Experiments can be manually controlled in labview based on specific requirements. The diameter of each sample was measured with an optical microscope before the compression test. The force and displacement data were collected, and the loading curve was plotted for further analysis. To characterize the failure strength of the core-shell structure, the nominal strength is defined as follows,

$$\sigma_n = \frac{F_m}{A} \tag{8}$$

where σ_n is the nominal strength, F_m is the maximum force at the rupture point and A is the initial cross-sectional area at the equator of a microcapsule. The deformation of the microcapsule can be calculated by the following equation,

$$\varepsilon = \frac{\delta d}{D} \tag{9}$$

where ε is the deformation, δ_d and D are the displacement and diameter, respectively.

2.5. Finite element method simulations

Given the symmetrical characteristic of the core-shell structure, an axisymmetric model was developed in Abaqus 6.14 to simulate the compression of a spherical microcapsule between two parallel flat plates. Two compression plates are analytical rigid. The shell of the microcapsule is meshed with five-layer CAX8R (8-node biquadratic axisymmetric quadrilateral, reduced integration) solid elements. The shell thickness h is 2 μm. In quasi-static compression, the liquid core generates a uniformly distributed hydrostatic pressure on the inner surface of the shell. Hence, the core was modelled as a fluid cavity. The density and bulk modulus of paraffin oil are 0.83 g/cm^3 and 1.66 GPa, respectively. The contact between the plates and the microcapsule was assumed to be frictionless and hard. The constitutive model for the shell material used here is elastic-perfectly plastic. The elastic modulus E and yield strength σ_Y were modified to fit the uniaxial compression data. The Poisson's ratio was defined as 0.33 in this model. The top plate was subjected to a displacement-controlled load.

3. Results and discussion

3.1. Characterization of fabricated PUF microcapsules

As can be seen in Fig. 1(a,b), morphology of PUF microcapsules was characterized by SEM. Few capsules not fully filled have a wrinkled surface as indicated by the red arrow. The outer surface of the PUF shell is much rougher than the inner surface [36], seen in Fig. 1(b,c). Agglomerates and clusters of nanoparticles randomly scattered on the outer surface due to synthesis process [48]. The dimension of these imperfections is hundreds of nanometers. They can create a good bonding condition when microcapsules are added into matrix materials. Meanwhile, the surface roughness tends to significantly affect the contact properties between the microcapsule and compression plates, especially in the first several microns. Microcapsules of different sizes were ruptured by a razor and the thickness of them was measured. It is found that the shell thickness of this batch of PUF microcapsules is about 2 μm, not uniform and independent of size, which is consistent with the published literature [21,36,48]. Fig. 1d shows the diameters of 300 microcapsules collected in Image J.

3.2. Mechanical properties

To characterize the intrinsic mechanical properties of the shell material of a microcapsule, nanoindentation test and uniaxial compression test were conducted on shell fragments and single microcapsules, respectively. The collected force-displacement data from compression test was fitted with FEM results. Furthermore, the structural deformation of a compressed microcapsule and the stress distribution in the shell was investigated numerically. To clearly elucidate the contribution of the liquid core and the solid shell to the mechanical response of the whole structure, parameter study of shell thickness to radius ratio (h/R) and bulk modulus of liquid (K) were carried out.

3.2.1. Modulus obtained from nanoindentation test

The size of the hardened cylindrical specimen was 3 cm in diameter and 1 cm in thickness as shown in Fig. 2a. Fig. 2(b,c) illustrates nanoindentation conducted on the inner surface of a PUF fragment embedded in an epoxy matrix. The relationship of force and displacement for four samples can be found in Fig. 2d. Nanoindentation test yields similar loading-unloading curves. All the samples show obvious stress relaxation during the holding stage due to the viscoelasticity of the shell material. For simplification, time-dependent behaviors are not considered in this work. Low ratio of indentation depth to shell thickness (10%) and hard epoxy substrate (~4.20 GPa) ensures that the experimental result is substrate-independent [44,49]. Through analyzing the initial unloading part of the curve as expressed in 2.3, the obtained E_r is 3.90 ± 0.26 GPa. Assuming the Poisson's ratio of PUF is 0.33, the Young's modulus is accordingly 3.48 ± 0.23 GPa.

According to the literature, the majority of researchers carried out nanoindentations on the intact microcapsules to extract its elastic properties [18–21,50]. To minimize the effect of the liquid core and structural deformation, the indentation depth is much smaller than shell thickness. However, the imperfections including nanoparticles, agglomerates and holes distributed on the outer surface make it hard to find a locally flat region to perform indentation. Jiang et al. [51] found that surface roughness can significantly influence the elastic modulus determined from nanoindentation tests. To eliminate the effect of surface morphology, the indentation depth needs to be much larger than the roughness dimension. Given that the real size of outer surface roughness is comparable with shell thickness, nanoindentation conducted on the smooth inner surface can provide more accurate and reliable experimental data.

3.2.2. Modulus and yield strength obtained from quasi-static compression test

Single microcapsules of different sizes were compressed until entirely collapsed to analyze their mechanical response in a wide deformation range. Afterwards, the experimental data was fitted with a numerical core-shell model based on different assumptions of constitutive models of the shell material.

Fig. 3a illustrates the quasi-static uniaxial compression of a single microcapsule. An obtained typical loading curve of PUF microcapsule is

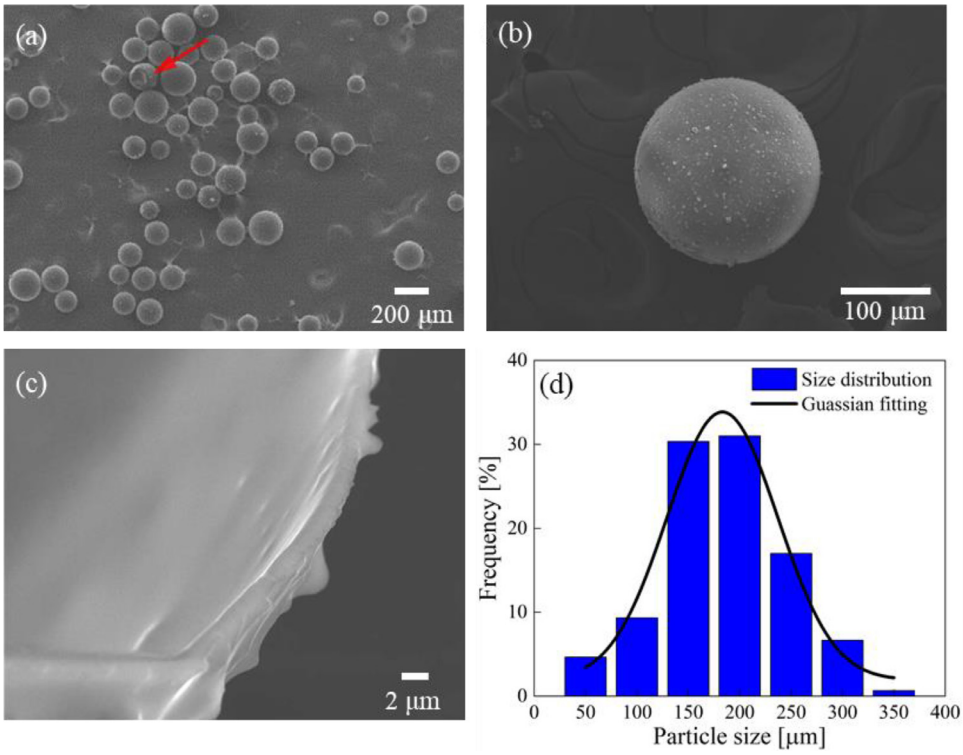

Fig. 1. (a,b) Morphology of PUF microcapsules, (c) shell structure and (d) distribution of PUF microcapsule size. Majority of the PUF microcapsules are fully filled with a rough outer surface.

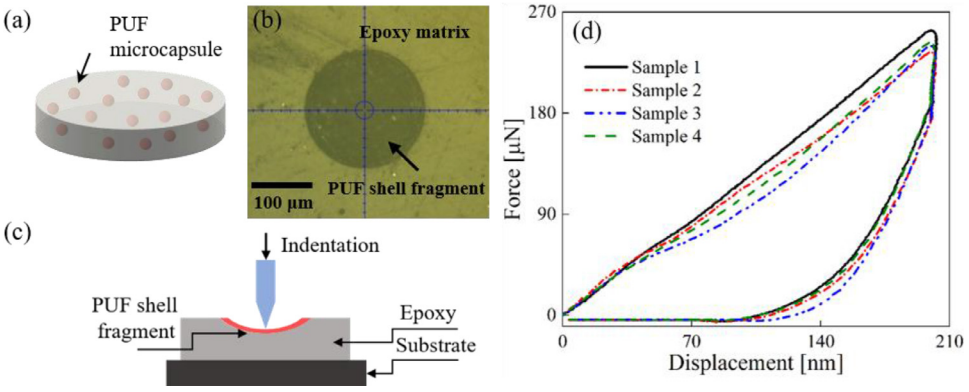

Fig. 2. (a) The cylindrical specimen before polished. PUF microcapsules are randomly distributed in the epoxy matrix. (b) An exposed PUF shell fragment embedded in the polished specimen. (c) Schematic of nanoindentation on the inner surface of PUF shell. The indentation was conducted at the polar region. (d) Force-displacement curves of nanoindentation for four samples. The elastic modulus was calculated from the initial linear unloading portion.

shown in Fig. 3b. Under 1 μm/s load, a microcapsule underwent four deformation stages: contact, flattened, initial failure and post-failure. At the first stage, the top compression plate touched the microcapsule. The circular contact region between the outer surface and the parallel plates expanded until the failure of the shell occurred. As being flattened, the shell material experienced the transmission from elasticity to plasticity. The failure of the shell initiated at the apex of the loading curve. The corresponding failure force and displacement are 18.8 mN and 51.6 μm, respectively. The calculated nominal strength and deformation are 0.42 MPa and 21.5% according to Eqs. (8) and (9). Following fluctuations on the curve indicates a more complex failure mechanism compared to a sudden drop of the load reported in the literature [26,37]. The almost intact microcapsule still remained its deformation resistance after initial failure. In the post-failure stage, the microcapsule gradually lost its load capacity and was entirely flattened. The encapsulated fluid was observed to leak out and covers both the shell surface and contact region.

As plastic deformations can be observed even at small displacements through simulation results, the loading curve before the failure point was fitted with FEM results, as shown in Fig. 3(c,d). As the displacement reaches approximately 12 μm, the pure elastic simulation result deviates from the compression data, as presented in Fig. 3c. It indicates that after fractional deformation of 5%, plasticity gradually becomes remarkable. Based on fitting at least five loading curves of microcapsules with different sizes, the obtained Young's modulus and yield strength are 3.50 ± 0.20 GPa and 40 ± 5 MPa, respectively.

3.2.3. *Nominal strength*

The nominal strength of PUF microcapsules of varying sizes calculated using Eq. (8) can be found in Fig. 4. The index obtained from power law fitting is −0.95. Smaller microcapsules tend to be stronger than larger ones. This trend can be explained by the higher shell thickness to radius ratio h/R of smaller microcapsules. The solid shell mainly undertakes the external loads and contributes to the overall strength. Additionally, since the larger ones can sustain higher loads, the imperfections in the shell including pores and agglomerates can lead to serious local stress concentrations which benefits the initiation and propagation of microcracks. This suggests that larger microcapsules may be more sensitive to imperfections in the shell. The calculated nominal strength shows a large degree of dispersion. This is mainly attributed to the imperfections in the shell and non-spherical geometry of fabricated microcapsules.

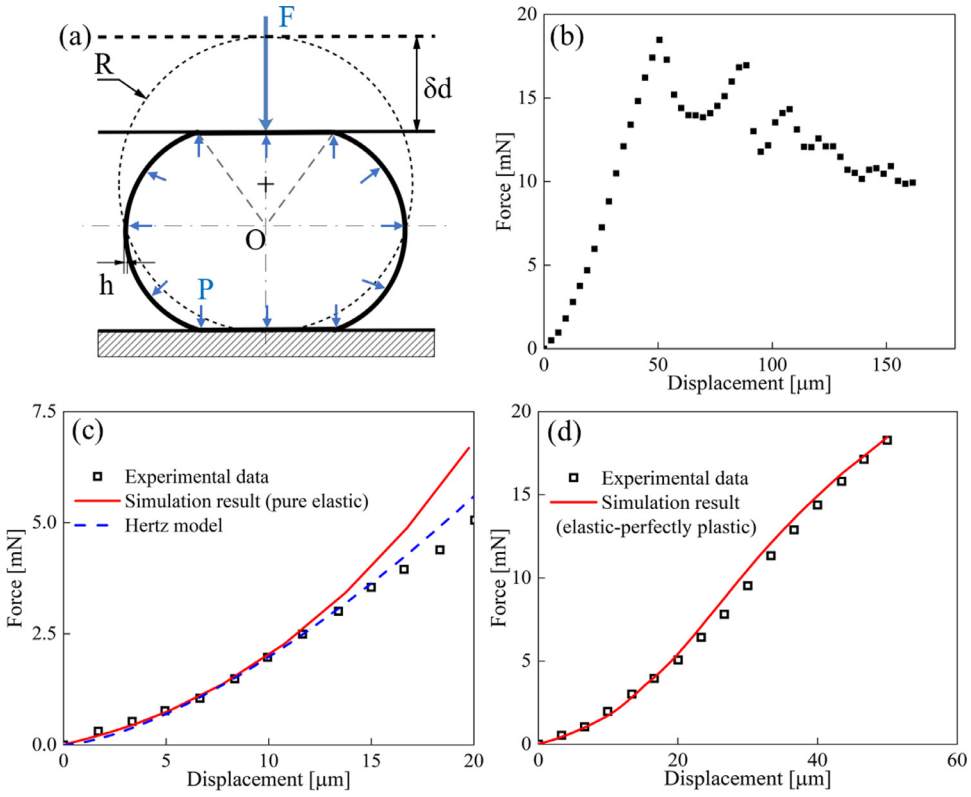

Fig. 3. (a) Scheme of a compressed microcapsule by two parallel rigid plates. Generated hydrostatic pressure P is uniformly distributed on the inner surface of the shell. (b) Force-displacement curve for compressing a PUF microcapsule of 240 μm in diameter. (c) The initial loading portion fitted with simulation result and Hertz solution for pure elastic shell. (d) Fitting result for the elastic-perfectly plastic shell. The obtained yield stress is 40 MPa.

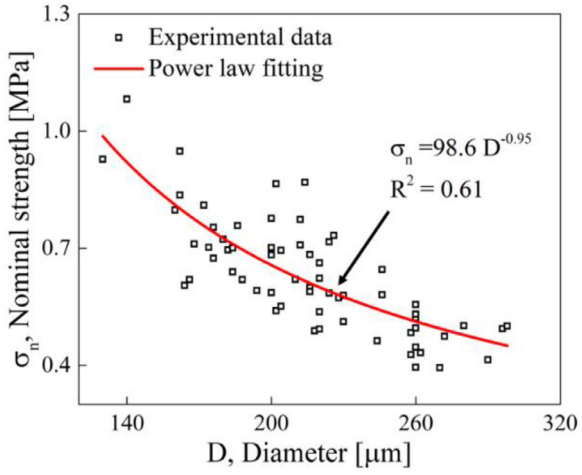

Fig. 4. Power law fitting of nominal strength of PUF microcapsules of varying sizes.

3.3. FEM analysis

3.3.1. Stress distribution and shell deformation

As a composite structure, a microcapsule presents different deformation features with stress evolution in the solid shell during being compressed. After the probe contacts the shell, high stress occurs at the outer surface within the circular contact region. When the total deformation reaches 0.02, the contacted area undergoes plastic deformation as illustrated in Fig. 5a. Meanwhile, the edge of the contact area is curved inward, resulting in a rising stress level. Since the plastic deformation is locally restricted at the contact, this limited plasticity cannot make a difference to the elastic response of the whole structure. As the shell is flattened, the yielded contact region and contact edge expand as shown in Fig. 5b. The initially arising noticeable yielding of a microcapsule on the loading curve is usually composed of these two parts. The entire shell almost yields at $\varepsilon = 0.2$. Fig. 5(d–f) presents the normal stresses at this stage. As can be seen, σ_{xx} is negative, which indicates that the non-contact region is subjected to compressive stress in the X direction contributed from the inner pressure of the core and shell bending. The stretching of the shell dominates at large deformations due to high tensile stresses in the Y and Z direction. Stresses in three directions lead to shell thinning, weakening the structure at the same time. Especially, stress at the equator increases quadratically for a pure elastic scenario as presented in Fig. 6. The blue line indicates that the plasticity at the equator emerges when deformation reaches about 0.1. And the non-contact area completely yields at $\varepsilon = 0.2$ approximately. Overall, the deformation of a microcapsule under compression is closely related to its core-shell structure. The change of a microcapsule's geometry tends to reduce the volume inside the shell. On the other hand, the mechanical response of the shell is to keep the volume constant due to the low compressibility of the liquid core. Thus, the contributions of the solid and liquid parts during deformation need further investigation.

3.3.2. The effect of shell thickness to radius ratio h/R

As a microcapsule containing liquid has a core-shell structure [52], studying the mechanical response of a microcapsule as a homogeneous sphere may bring about erroneous results. To comprehensively understand the microcapsule mechanics, the effect of the shell thickness to radius ratio h/R as a key geometrical parameter needs to be clarified. As can be seen in Fig. 7, the normalized force F/EhR increases linearly with the ratio h/R at a small deformation ($\varepsilon = 5\%$) for thin-walled microcapsules ($h/R \leq 0.2$). Consequently, the total reaction force is

$$F = K_1 \cdot Eh^2 + K_2 \cdot EhR \tag{10}$$

where K_1 is the slope and K_2 is the intercept of the fitting line. They are functions of deformation and Poisson's ratio of the shell material [53]. For thick-walled microcapsules, no such relationship has been found. Two terms of Eq. (10) express the bending effect and stretching effect,

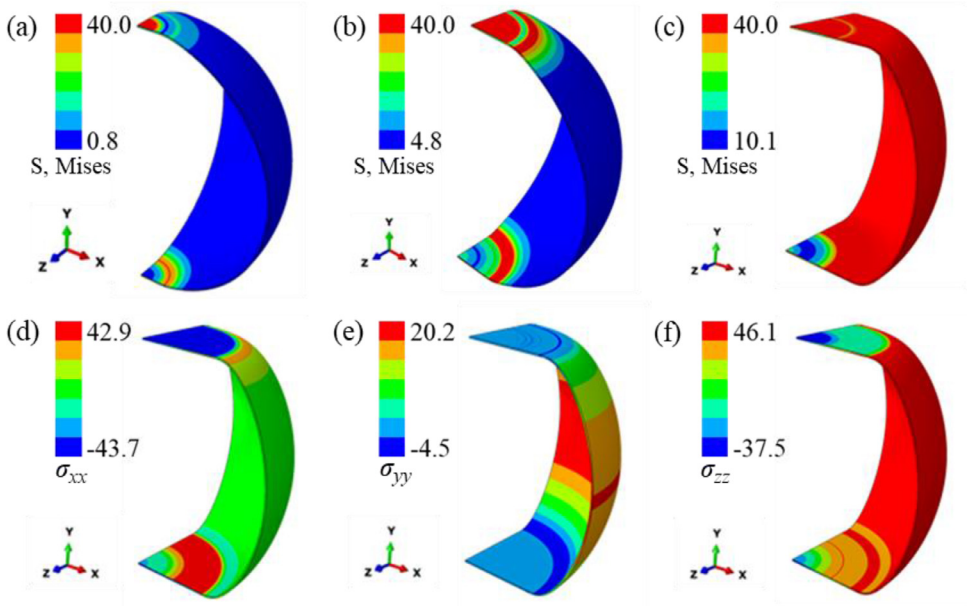

Fig. 5. Von Mises stress nephogram in the shell (h/R = 1%) at different deformations (σ_Y = 40 MPa): (a) ε = 0.02, (b) ε = 0.05 and (c) ε = 0.2. (d–f) Normal stresses σ_{xx}, σ_{yy} and σ_{zz} at deformation ε = 0.2. (Units: MPa).

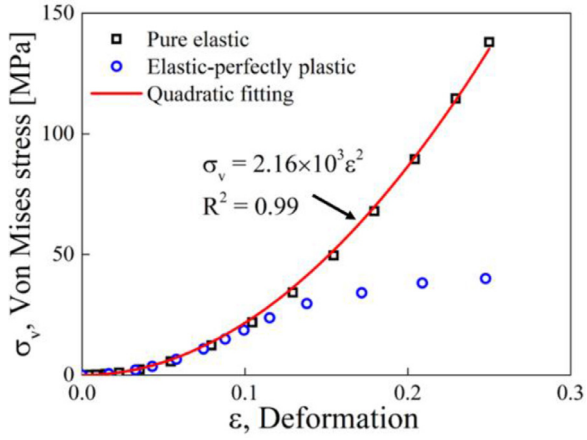

Fig. 6. Von Mises stress value at the shell equator for pure elastic and elastic-perfectly plastic simulations.

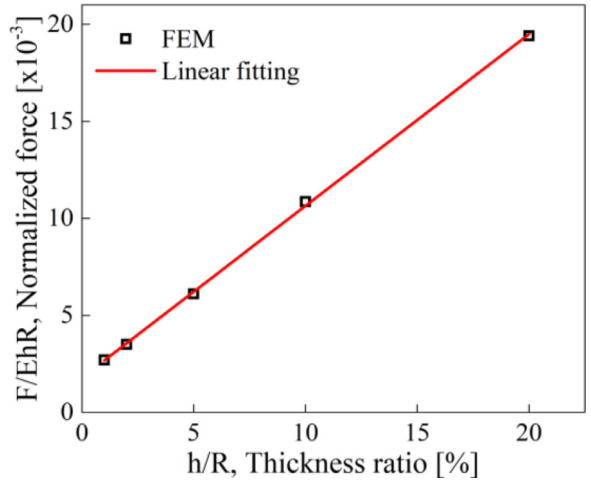

Fig. 7. Normalized force F/EhR versus shell thickness to radius ratio h/R. The normalized force F/EhR increases linearly with the ratio h/R at a small deformation (ε = 5%).

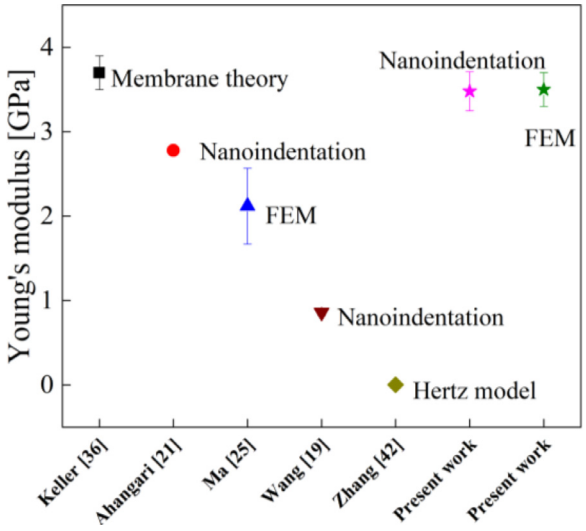

Fig. 8. Comparison of present work with literature for Young's modulus estimation of PUF microcapsules. The discrepancy is mainly due to different applied models and experimental methods. Present results using two methods has shown great consistence.

respectively. Their importance can be analyzed according to the ratio of them $K = K_1/K_2 \bullet h/R$ [54]. Reissner neglected stretching deformation and obtained Eq. (4) for hollow thin-walled spherical shells. However, if the ratio h/R is sufficiently small, a microcapsule encapsulating liquid can be considered as a fluid-filled membrane. The stretching effect dominates in this regime and the bending resistance of the shell can be safely neglected. As a result, even for thin-walled microcapsules, Reissner's model may give inaccurate predictions.

Fig. 8 presents the estimation of Young's modulus for PUF microcapsules in literature. Keller followed the membrane theory model developed by Lardner and Pujara [55] which neglected the bending resistance of the shell. Ahangari and Wang performed nanoindentation tests on PUF microcapsules and determined the mechanical properties of the shell. Although they used the same method based on elastic theory to solve this problem at small deformations, they have obtained different values. The reason can be explained as different shell compositions due

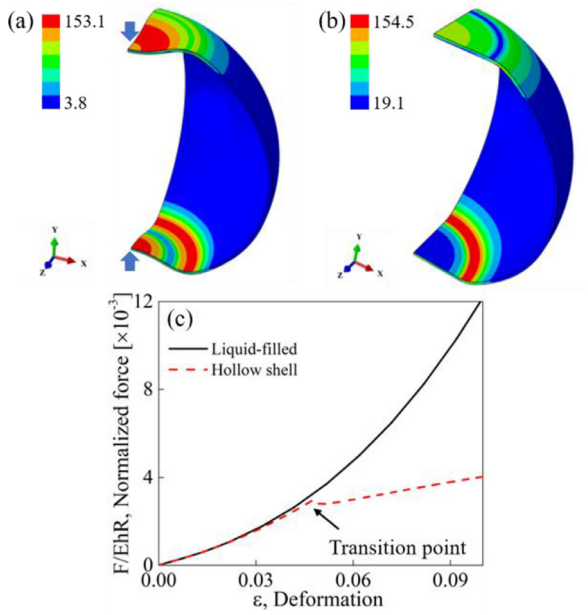

Fig. 9. Von Mises stress nephogram in the shell (units: MPa) for (a) a hollow shell and (b) a liquid-filled microcapsule at deformation $\varepsilon = 0.1$, (c) comparison of F/EhR - ε curves from elastic simulation ($h/R = 2\%$). The hollow shell buckles as the deformation reaches 4.8% while the liquid-filled shell remains flattened configuration.

to synthesis and experimental errors brought about by surface roughness. Ma and Zhang conducted quasi-static compression on individual microcapsules and analyzed the data by comparison with FEM results and the Hertz model, respectively. Meanwhile, the blue line in Fig. 3c indicates that the calculated modulus from Hertz solution is 10.8 MPa ($\delta_d = 2\Delta$). For a core-shell structured microcapsule compressed slowly by two parallel plates, the elastic modulus obtained from the Hertz solution is about three orders lower than that from nanoindentation (3.48 GPa) and numerical simulation (3.50 GPa). Unless the deformation of a thin-walled microcapsule is sufficiently small, the encapsulated liquid core can dramatically soften the whole structure compared to a solid sphere, resulting in an underestimated apparent modulus.

3.3.3. The effect of the liquid core

The mechanical response of microcapsules under compression is a process of two-way fluid-solid coupling. The effect of liquid core's surface tension is not considered in this work [56]. The inner pressure P affects the stress state of the shell and prevents it from buckling inward compared to hollow shells [57]. As shown in Fig. 9a, a hollow thin shell buckles after being flattened. The transition from the flattened to the buckled configuration happens at $\varepsilon = 4.8\%$, as presented in Fig. 9c. The stiffness of the shell declines dramatically after buckling. The volume inside the buckled shell greatly decreases. This nonlinear process can be analyzed from the perspective of minimizing the elastic energy of the shell [57]. Nevertheless, no buckling can be found in the liquid-filled microcapsule due to the low compressibility of the liquid core. Thus, the existence of encapsulated liquid enhances the stability of the whole structure before it ruptures. It can be predicted that the stability and stiffness of a microcapsule could be much lower than prospected if it is not fully filled.

In quasi-static compression of a microcapsule, the fluid is considered as static without motions. Since the inertia effect is not taken into account, the hydrostatic pressure generated by liquid core can be written as

$$P = -K \cdot \frac{\Delta V}{V_0} \tag{11}$$

where P is the generated inner pressure, K is the bulk modulus of liquid, ΔV is the volume change and V_0 is the initial volume of the liquid core. As a fluid-structure interaction problem [58], the slightly deformed liquid core generates a hydrostatic pressure when the solid shell deforms due to external loads as depicted in Fig. 3a. The pressure is uniformly distributed on the inner surface of the shell. Different from a solid medium, no stress concentration emerges in the liquid core. Modeling it as a solid core makes this problem easier to solve numerically but harder to correctly understand. The encapsulated liquid material was usually considered as incompressible in the previous research due to the low compressibility of liquid. To investigate the influence of bulk modulus, different values of K ranging from 1.0~5.0 GPa were selected for pure elastic simulation. As presented in Fig. 9a, the reaction force is more sensitive to the bulk modulus of the liquid core at larger deformations. At deformation $\varepsilon = 0.5$, the force rises by 3.3% with K increasing from 1.0 to 5.0 GPa. This can be explained by the severely compressed core due to large structural deformations of the shell. While at the initial compression stage, deformation is restricted at the contact region between the probe and the shell. The contribution of the core is negligible since it is almost not compressed. With increasing structural deformation of the shell, the inner pressure goes up due to the gradually compressed liquid core. Although the volume change fraction of core is far less than 1% in these simulations, the hydrostatic pressure and deformation have shown a strong correlation with each other as presented in Fig. 10b. The inner pressure is normalized by the bulk modulus of the liquid and it is found to increase with the total deformation in a quadratic manner. It can be observed that P/K increases slowly for $\varepsilon \leq 0.1$ and climbs fast then. Thus, the core effect matters especially at large structural deformations and the corresponding high inner pressure contributes to the mechanical response of the solid shell in many ways including shell stretching and shell stability.

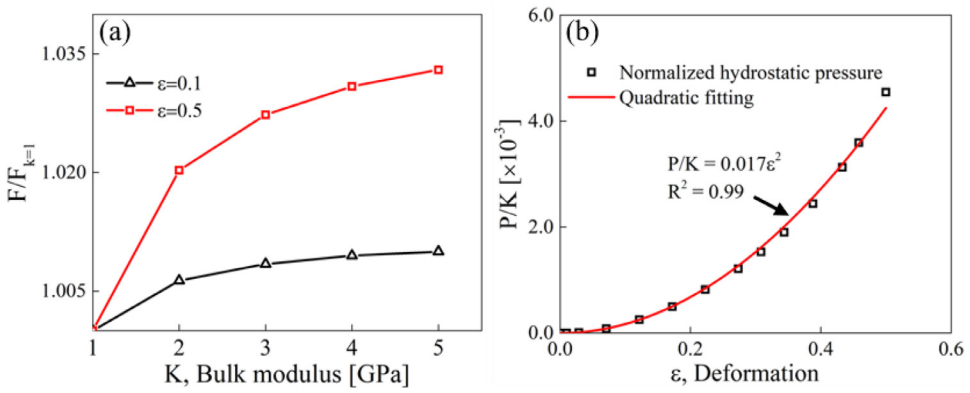

Fig. 10. (a) Normalized force $F/F_{k=1}$ as a function of bulk modulus of the liquid core at deformation $\varepsilon = 0.1$ and $\varepsilon = 0.5$. The bulk modulus makes a stronger impact at a larger deformation. (b) Quadratic fitting of normalized hydrostatic pressure in the liquid core for thin-walled microcapsules ($h/R = 1\%$).

4. Conclusions

The main purpose of this work is to analyze the effect of liquid core on the mechanical behaviors of a microcapsule under compression. The intrinsic mechanical properties of the solid shell are successfully extracted through two experimental techniques for the first time. The mechanical response of a microcapsule differs in different deformation stages due to interaction of the core-shell structure. The following conclusions are drawn.

1 Nanoindentation tests on the inner smooth surface of PUF shell fragments embedded in epoxy provide the Young's modulus of 3.48 ± 0.23 GPa. The Young's modulus and yield strength extracted from quasi-static compression data are 3.50 ± 0.20 and 40 ± 5 MPa, respectively. Smaller microcapsules are found to be stronger than their larger counterparts as a result of a higher thickness ratio and less sensitivity to imperfections in the shell.
2 The structure-mechanical relationship of a core-shell structure is revealed using FEM. With increasing structural deformation, high stresses expand from circular contact area to non-contact area. At small deformations, F/EhR increases linearly with h/R which indicates the contribution of bending and stretching of the shell. Reissner's model neglects stretching force which matters for liquid-filled membrane. Hertz solution dramatically underestimates the modulus of the shell material for a thin-walled microcapsule due to the compliant liquid core.
3 The existence of the liquid core can affect the mechanical performance of the whole composite structure in many ways. At large deformations, the liquid core's low compressibility leading to high hydrostatic inner pressure can effectively prevent the shell from buckling inward and facilitate the stretching of the non-contact part.

Quasi-static mechanical properties of single thin-walled microcapsules are studied by various means. This work is significant for guiding the design and application of new types of microcapsules. The mechanical behaviors of microcapsules added into a matrix, the effect of liquid core in high-rate compressions and the shell failure mechanism may need more investigations to comprehensively understand microcapsule mechanics.

Declaration of Competing Interest

The authors declare no conflict of interest.

CRediT authorship contribution statement

Yunxiao Zhang: Writing – review & editing, Methodology, Investigation, Software, Formal analysis. **Ying Zhao:** Investigation. **Fang Wu:** Methodology, Writing – review & editing. **Xin Zhang:** Methodology, Writing – review & editing. **Zhong Zhang:** Funding acquisition, Writing – review & editing. **Yong Xiang:** Funding acquisition, Writing – review & editing. **Jinglei Yang:** Resources, Writing – review & editing, Supervision, Project administration, Funding acquisition.

Acknowledgments

The authors are grateful for the support from The Hong Kong University of Science and Technology (Grants #: R9365, R6381) and the NSFC-RGC/HK Joint Research Scheme (Grants#: N_HKUST 631/18 and 51861165103).

References

[1] Jong HGBD. Die Koazervation und ihre Bedeutung für die Biologie. Protoplasma 1932;15(1):110–73.
[2] Jong HGBD, Bonner J. Phosphatide auto-complex coacervates as ionic systems and their relation to the protoplasmic membrane. Protoplasma 1935;24(24):198–218.
[3] Dai LH, Ling Z, Bai YL. Size-dependent inelastic behavior of particle-reinforced metal–matrix composites. Compos Sci Technol 2001;61(8):1057–63.
[4] Youan BBC, Jackson TL, Lorenzo D, Carmen H, Owusu-Ababio G. Protein release profiles and morphology of biodegradable microcapsules containing an oily core. J Control Release 2001;76(3):313–26.
[5] Madene A, Jacquot M, Scher J, Desobry S. Flavour encapsulation and controlled release–a review. Int J Food Sci Technol 2005;41(1):1–21.
[6] Khun NW, Zhang H, Yue CY, Yang JL. Self-lubricating and wear resistant epoxy composites incorporated with microencapsulated wax. J Appl Mech 2014;81(7):071004.
[7] Wu G, An JL, Tang XZ, Xiang Y, Yang JL. A versatile approach towards multifunctional robust microcapsules with tunable, restorable, and solvent-proof superhydrophobicity for self-healing and self-cleaning coatings. Adv Funct Mater 2014;24(43):6751–61.
[8] Zhang W, L Q, Pei H, Qin Z, Didier J, Wu Z, et al. Controllable fabrication of inhomogeneous microcapsules for triggered release by osmotic pressure. Small 2019;15(42):1903087.
[9] Bah MG, Bilal HM, Wang JT. Fabrication and application of complex microcapsules: a review. Soft Matter 2020;16(3):570–90.
[10] Bansode S, Banarjee S, Gaikward DD, Jadhay S, Thorat RM. Microencapsulation: a review. Int J Pharm Sci Rev Res 2010;1(2):38–43.
[11] Mercadé-Prieto R, Zhang ZB. Mechanical characterization of microspheres–capsules, cells and beads: a review. J Microencapsul 2012;29(3):277–85.
[12] Neubauer MP, Poehlmann M, Fery A. Microcapsule mechanics: from stability to function. Adv Colloid Interface Sci 2014;207:65–80.
[13] Gray A, Egan S, Bakalis S, Zhang ZB. Determination of microcapsule physicochemical, structural, and mechanical properties. Particuology 2016;24:32–43.
[14] Pham ST, Tieu KA, Wan S, Hao J, Nguyen HH, Mitchell DRG, et al. Intrinsic effect of nanoparticles on the mechanical rupture of doubled-shell colloidal capsule via *in situ* TEM mechanical testing and STEM interfacial analysis. Small 2020;16(29):2001978.
[15] Sarrazin B, Tsapis N, Mousnier L, Taulier N, Urbach W, Guenoun P. AFM investigation of liquid-filled polymer microcapsules elasticity. Langmuir 2016;32(18):4610–18.
[16] Du MM, Kavanagh D, Kalia N, Zhang ZB. Characterising the mechanical properties of haematopoietic and mesenchymal stem cells using micromanipulation and atomic force microscopy. Med Eng Phys 2019;73:18–29.
[17] Delcea M, Schmidt S, Palankar R, Fernandes PAL, Fery A, Mohwald H, et al. Mechanobiology: correlation between mechanical stability of microcapsules studied by AFM and impact of cell-induced stresses. Small 2010;6(24):2858–62.
[18] Su JF, Wang XY, H D. Micromechanical properties of melamine–formaldehyde microcapsules by nanoindentation: effect of size and shell thickness. Mater Lett 2012;89:1–4.
[19] Wang XF, Han R, Han TL, Han NX, Xing F. Determination of elastic properties of urea-formaldehyde microcapsules through nanoindentation based on the contact model and the shell deformation theory. Mater Chem Phys 2018;215:346–54.
[20] Ren YM, Abbas N, Zhu GM, Tang JN. Synthesis and mechanical properties of large size silica shell microcapsules for self-healing cementitious materials. Coll Surf A Physicochem Eng Asp 2020;587:124347.
[21] Ahangari MG, Fereidoon A, Jahanshahi M, Sharifi N. Effect of nanoparticles on the micromechanical and surface properties of poly (urea–formaldehyde) composite microcapsules. Compos Part B Eng 2014;56:450–5.
[22] Mercadé-Prieto R, Allen R, York D, Preece JA, Goodwin TE, Zhang Z. Determination of the failure stresses for fluid-filled microcapsules that rupture near the elastic regime. Exp Mech 2012;52(9):1435–45.
[23] Pan XM, York DY, Preece JA, Zhang ZB. Size and strength distributions of melamine–formaldehyde microcapsules prepared by membrane emulsification. Powder Technol 2012;227:43–50.
[24] Pan XM, Mercadé-Prieto R, York D, Preece JA, Zhang ZB. Structure and mechanical properties of consumer-friendly PMMA microcapsules. Ind Eng Chem Res 2013;52(33):11253–65.
[25] Ma WP, Zhang W, Zhao Y, Wang SJ. Estimation of the mechanical properties of urea–formaldehyde microcapsules by compression tests and finite element analysis. J Appl Polym Sci 2016;133(19):43414.
[26] Hu JF, Chen HQ, Zhang ZB. Mechanical properties of melamine formaldehyde microcapsules for self-healing materials. Mater Chem Phys 2009;118(1):63–70.
[27] Hertz H. Ueber die Berührung fester elastischer Körper. J. fur die Reine und Angew. Math. 1882;1882(92):156–71.
[28] Fischer-Cripps AC. The Hertzian contact surface. J Mater Sci 1999;34(1):129–37.
[29] Dintwa E, Tijskens E, Ramon H. On the accuracy of the Hertz model to describe the normal contact of soft elastic spheres. Granul Matter 2008;10(3):209–21.
[30] Pastewka L, Robbins M. Contact area of rough spheres: large scale simulations and simple scaling laws. Appl Phys Lett 2016;108(22):221601.
[31] Zhao JH, Nagao S, Zhang ZL. Loading and unloading of a spherical contact: from elastic to elastic–perfectly plastic materials. Int J Mech Sci 2012;56(1):70–6.
[32] Johnson KL, Kendall K, Roberts AD. Surface energy and the contact of elastic solids. Proc Math Phys Eng Sci 1971;324(1558):301–13.
[33] Reissner E. Stresses and small displacements of shallow spherical shells. II. J Math Phys 1946;25(1–4):279–300.
[34] Yu HY, Kongsmo R, Patil N, He JY, Breiby DW, Zhang ZL. On determining the Poisson's ratio of viscoelastic polymer microparticles using a flat punch test. Int J Mech Sci 2017:128–9 150-158.
[35] Kenner VH, Goldsmith W. Dynamic loading of a fluid-filled spherical shell. Int J Mech Sci 1972;14(9):557–68.
[36] Keller MW, Sottos NR. Mechanical properties of microcapsules used in a self-healing polymer. Exp Mech 2006;46(6):725–33.
[37] Yang JL, Keller MW, Moore JS, White SR, Sottos NR. Microencapsulation of isocyanates for self-healing polymers. Macromolecules 2008;41(24):9650–5.

[38] Mercade-Prieto R, Allen R, York D, Preece JA, Goodwin TE, Zhang ZB. Compression of elastic–perfectly plastic microcapsules using micromanipulation and finite element modelling: determination of the yield stress. Chem Eng Sci 2011;66(9):1835–43.
[39] Mercadé-Prieto R, Nguyen B, Allen R, York D, Preece JA, Goodwin TE, et al. Determination of the elastic properties of single microcapsules using micromanipulation and finite element modeling. Chem Eng Sci 2011;66(10):2042–9.
[40] Ghaemi A, Philipp A, Bauer A, Last K, Fery A, Gekle S. Mechanical behaviour of microcapsules and their rupture under compression. Chem Eng Sci 2016;142:236–43.
[41] Zhang X, Wang PF, Sun DW, Li X, Yu TX, Yang EH, et al. Rate dependent behaviors of nickel-based microcapsules. Appl Phys Lett 2018;112(22):221905.
[42] Zhang X, Wang PF, Sun DW, Li X, An JL, Yu TX, et al. Dynamic plastic deformation and failure mechanisms of individual microcapsule and its polymeric composites. J Mech Phys Solids 2020;139:103933.
[43] Sun DW, Chong YB, Chen K, Yang JL. Chemically and thermally stable isocyanate microcapsules having good self-healing and self-lubricating performances. Chem Eng J 2018;346(15):289–97.
[44] Tsui TY, Pharr GM. Substrate effects on nanoindentation mechanical property measurement of soft films on hard substrates. J Mater Res 1999;14(1):292–301.
[45] Zha XM, Jiang F, Xu XP. Investigation of modelling and stress distribution of a coating/substrate system after an indentation test. Int J Mech Sci 2017;134:1–14.
[46] Oliver WC, Pharr GM. An improved technique for determining hardness and elastic modulus using load and displacement sensing indentation experiments. J Mater Res 1992;7(6):1564–83.
[47] Pharr GM, Oliver WC, Brotzen FR. On the generality of the relationship among contact stiffness, contact area, and elastic modulus during indentation. J Mater Res 1992;7(3):613–17.
[48] Cosco S, Ambrogi V, Musto P, Carfagna C. Properties of poly (urea-formaldheyde) microcapsules containing an epoxy resin. J Appl Polym Sci 2007;105(3):1400–11.
[49] Box F, Jacquemot C, Adda-Bedia M, Vella D. Cloaking by coating: how effectively does a thin, stiff coating hide a soft substrate? Soft Matter 2020;16(19):4574–83.
[50] Sohail T, Nadler B. On the indentation of a fluid-filled spherical particle. Int J Mech Sci 2013;75:305–15.
[51] Jiang WG, Su JJ, Feng XQ. Effect of surface roughness on nanoindentation test of thin films. Eng Fract Mech 2008;75(17):4965–72.
[52] Li YQ, Gao XL, Horner SE, Zheng JQ. Analytical models for the impact of a solid sphere on a fluid-filled spherical shell incorporating the stress wave propagation effect and their applications to blunt head impacts. Int J Mech Sci 2017;130:586–95.
[53] Lulevich VV, Andrienko D, Vinogradova OI. Elasticity of polyelectrolyte multilayer microcapsules. J Chem Phys 2004;120(8):3822–6.
[54] Dai Z, Lu N. Poking and bulging of suspended thin sheets: slippage, instabilities, and metrology. J Mech Phys Solids 2021;149:104320.
[55] Lardner TJ, Pujara P. Compression of spherical cells. mechanics today. Elsevier; 1980. p. 161–76.
[56] Rao Y, Qiao S, DAi Z, Lu N. Elastic wetting: substrate-supported droplets confined by soft elastic membranes. J Mech Phys Solids 2021;151:104399.
[57] Pauchard L, Rica S. Contact and compression of elastic spherical shells: the physics of a 'ping-pong'ball. Philos Mag B 1998;78(2):225–33.
[58] Majid S, Funnell WRF. Mechanical behaviour of short membranous liquid-filled cylinders under axial loadings. Int J Mech Sci 2018;145:138–44.